



Idiosyncratic epistasis creates universals in mutational effects and evolutionary trajectories

Daniel M. Lyons ^{1,2}, Zhengting Zou ^{1,2}, Haiqing Xu ¹ and Jianzhi Zhang ¹ ✉

Patterns of epistasis and shapes of fitness landscapes are of wide interest because of their bearings on a number of evolutionary theories. The common phenomena of slowing fitness increases during adaptations and diminishing returns from beneficial mutations are believed to reflect a concave fitness landscape and a preponderance of negative epistasis. Paradoxically, fitness decreases tend to decelerate and harm from deleterious mutations shrinks during the accumulation of random mutations—patterns thought to indicate a convex fitness landscape and a predominance of positive epistasis. Current theories cannot resolve this apparent contradiction. Here, we show that the phenotypic effect of a mutation varies substantially depending on the specific genetic background and that this idiosyncrasy in epistasis creates all of the above trends without requiring a biased distribution of epistasis. The idiosyncratic epistasis theory explains the universalities in mutational effects and evolutionary trajectories as emerging from randomness due to biological complexity.

Epistasis, or genetic interaction among a set of mutations, impacts the phenotypic effects of mutations and shapes fundamental evolutionary processes¹. Epistasis is said to be positive (or negative) for a particular trait such as fitness if the trait value of the individual with multiple mutations is greater (or smaller) than the expectation from the corresponding single mutants under no epistasis¹. A number of evolutionary theories, such as the mutational deterministic hypothesis of the evolution of sexual reproduction² and the hypothesis of reduction in mutational load by truncation selection against deleterious mutations, depend on assumptions of general trends of epistasis³. Universal patterns involving epistasis are emerging from decades of intense investigations^{4,5}. For instance, many experimental evolution studies have shown that fitness increase slows during organismal adaptation to a constant environment⁶. While the speed of fitness increase is typically measured per unit time⁶, the same trend is observed when the speed is measured per mutation accrued⁷. This phenomenon of slowing adaptation is at least in part due to diminishing-returns epistasis—a common observation that advantageous mutations are less beneficial on fitter genetic backgrounds^{8–11}. Because diminishing-returns epistasis is a form of negative epistasis, the above observations are thought to indicate a preponderance of negative epistasis between beneficial mutations and a concave fitness landscape¹². Given the concave shape of the landscape inferred from ascent to a fitness peak, one would also expect to observe a concave shape during descent from the fitness peak (that is, accelerating fitness decline by mutation accumulation and negative epistasis between deleterious mutations). In contrast with this expectation, mutation accumulation experiments in the near absence of selection have revealed decelerating fitness declines^{13–15}, and manipulative experiments have demonstrated that deleterious mutations tend to be less harmful in less fit genetic backgrounds (also known as increasing-costs epistasis because of the higher costs of deleterious mutations in fitter genotypes)¹⁶. These observations concerning deleterious mutations are thought to indicate a convex fitness landscape and a predominance of positive epistasis^{12,13}.

Apparently, the inferred shape of the fitness landscape and distribution of epistasis from climbing fitness peaks contrast with the shape and distribution inferred from going down fitness peaks¹². Consider a restatement of the problem. Mutation accumulation and manipulative experiments suggest that the majority of mutational paths down a fitness peak are convex (positively epistatic). Thus, most mutational pathways up the peak during adaptation should be convex as well (positively epistatic), but the opposite is observed. We term this contradiction the uphill–downhill paradox.

Although several theoretical models have been proposed to explain the inferred prevalence of either negative or positive epistasis^{9,10,13,16–20}, these models cannot simultaneously explain both in the same species, leaving the uphill–downhill paradox unresolved. For instance, the modular life model explains the negative epistasis among beneficial mutations by functional saturation of modules¹⁷, but it also predicts negative epistasis among detrimental mutations. The metabolic control theory has been invoked in explaining the positive epistasis among deleterious mutations because a deleterious mutation in a linear pathway causes a smaller flux reduction when other enzymes in the pathway have already been adversely affected^{16,21}. However, this theory would also predict positive epistasis of beneficial mutations. Alternatively, one must additionally assume that adaptation is biased towards mutations that disrupt costly expendable pathways in order to explain diminishing returns¹². Clearly, this assumption cannot be generally true. Theoretical work making no mechanistic assumptions has shown some promise^{22,23}. Such work has found that pairwise epistasis between successive adaptive mutations is positively biased during late stages of adaptation, even in a landscape of no overall bias of epistasis, suggesting that the epistasis between beneficial mutations may not represent the overall epistasis in the landscape. However, how this finding relates to the observed epistasis trends in adaptation and mutation accumulation is unclear. Rather than assuming a specific biological mechanism, below we propose and demonstrate that epistasis is generally idiosyncratic and that this idiosyncrasy is responsible for the general trends in both climbing and descending from fitness peaks.

¹Department of Ecology and Evolutionary Biology, University of Michigan, Ann Arbor, MI, USA. ²These authors contributed equally: Daniel M. Lyons, Zhengting Zou. ✉e-mail: jianzhi@umich.edu

Results

Why epistasis could be highly idiosyncratic. Let g be the population growth rate (also known as Malthusian fitness, logarithm of Wrightian fitness or fitness for short) of a genotype in an environment and let n be the number of nucleotide sites in the genome that impact g . In general, g can be expressed as the sum of $2^n - 1$ terms of fitness effects, including the additive effect of every site, the interactive effect of every pair of sites, the interactive effect of every triplet of sites, and so on (see Methods). We refer to this model of fitness landscape as the n -order model, because it includes all terms up to the n -order interaction. It can be shown that a mutation at a single site changes up to $2^{n-1}/(2^n - 1) \approx 50\%$ of all terms of effects making up g . Under the assumption that the interactive terms are idiosyncratic (that is, varying with the interacting nucleotides involved), a single mutation can differentially alter as many as 2^{n-2} (or $\sim 25\%$) terms of effects in two genotypes that differ by only one nucleotide; this number can rise up to 2^{n-1} (or $\sim 50\%$) terms if the two genotypes are more different (see Methods). Given the potential of such a large fraction of differentially affected terms of g , it is not surprising that the same mutation could have vastly different effects in different genotypes. As long as the idiosyncrasy assumption holds, the same argument can be made for any phenotypic trait whose value is expressed as the sum of all additive and interactive terms of effects. Of course, not all $2^n - 1$ terms of effects are of the same magnitude, which would increase or decrease the effective fraction of terms differentially altered by a mutation. Regardless, the above consideration elucidates why mutational effects could be highly sensitive to the genetic background when biological interactions are complex.

Epistasis is highly idiosyncratic. To quantify the above sensitivity that originates from idiosyncratic epistasis, we define an idiosyncratic index (I_{id}) for a mutation as the variation in the fitness difference between genotypes that differ by the mutation, relative to the variation in the fitness difference between random genotypes for the same number of genotype pairs. Here, the variation may be measured by s.d., range or other statistics. We can further compute the I_{id} for a fitness landscape by averaging I_{id} of individual mutations considered. The I_{id} for a landscape varies from 0 to 1, corresponding to the minimum and maximum levels of idiosyncrasy, respectively. We first estimated I_{id} for the fitness landscape of a yeast transfer RNA (tRNA) gene that includes experimentally measured fitness of over 65,000 genotypes²⁴. For example, the G-to-A mutation at site 10 has a fitness effect varying from -0.53 to 0.29 (s.d. = 0.13) on 88 different backgrounds. For comparison, the fitness difference between a randomly picked genotype and another randomly picked genotype varies from -0.59 to 0.74 (s.d. = 0.26) for 88 genotype pairs sampled (Fig. 1a). So, the ratio of the two s.d. values is 0.49. This analysis was repeated for 828 single mutations (considering reverse mutations) (Fig. 1b) and the average ratio of s.d. is $I_{id} = 0.612 \pm 0.005$ (s.e.m.). I_{id} can be similarly defined for non-fitness traits, and we estimated I_{id} for a variety of empirical phenotype landscapes that are experimentally determined^{24–32} and one that is computationally predicted (RNA stability) (Supplementary Table 1). Overall, I_{id} varies from 0.18 to 0.80 among the 12 landscapes examined, with a mean of 0.43 (Fig. 1c). Hence, in an average phenotype landscape, a particular mutation's effects across different backgrounds are 43% as variable as if they are randomly drawn from the effects of any number of mutations on any genetic background. To exclude the possibility that the observed idiosyncrasy is largely due to imprecise phenotyping, we computed I_{id} for the same 828 mutations in the tRNA landscape, but used fitness estimates from different numbers of experimental replicates, because the measurement error should decrease with the number of replicates. We found that I_{id} is insensitive to the number of replicates (Extended Data Fig. 1a), suggesting that the high idiosyncrasy is not explained by potentially imprecise phenotyping. Additionally, phenotypic values in the RNA stability

landscape were computed deterministically without measurement error, but mutational effects are still one-quarter as idiosyncratic as the maximum ($I_{id} = 0.25$). We similarly observed high idiosyncrasy when the range instead of s.d. of effects was used in estimating I_{id} (Extended Data Fig. 1b). Finally, another measure of idiosyncrasy is the frequency of sign epistasis in a landscape, or the proportion of mutations that are beneficial in some backgrounds but detrimental in others. In agreement with the high idiosyncrasy indices, nearly all mutations exhibit sign epistasis in all landscapes (93.7% of mutations, on average) (Extended Data Fig. 1b).

Expected consequences of idiosyncratic epistasis. Below, we demonstrate the consequences of the substantial idiosyncrasy we find with regard to fitness, but the same applies to other traits. In a maximally idiosyncratic fitness landscape such as the one described by the house-of-cards model³³, fitness values (circle sizes in Fig. 1d) of neighbouring genotypes connected through single mutations are uncorrelated. The fitness of a neighbouring genotype of a high- or low-fitness focal genotype is expected to be the same. Hence, the fitness difference between a neighbouring genotype (grey circle) and the focal genotype (black circle) is expected to be less positive or more negative as the fitness of the focal genotype rises. In other words, beneficial mutations are less beneficial and deleterious mutations are more deleterious on fitter genotypes, causing diminishing returns and increasing costs, respectively. These arguments apply not only to the effects of the same mutation on different genetic backgrounds but also to the effects of different mutations on different backgrounds. That is, an arbitrary mutation on a relatively fit background is expected to be less beneficial or more detrimental than another arbitrary mutation on a relatively unfit background. Under the foregoing model of g , one can mathematically prove that, in the presence of idiosyncrasy of at least one interactive term, the correlation between the fitness effect of a mutation and the background fitness is negative, for both the same and different mutation(s) (see Methods). In the case of different mutations, among-site or among-state variation in the additive effect further contributes to the negative correlation (see Methods). Importantly, all of the above occurs even with no bias towards positive or negative epistasis in the fitness landscape and no fitness estimation error.

Idiosyncratic epistasis causes the trends of diminishing returns and increasing costs. To examine whether the extent of idiosyncratic epistasis in an actual fitness landscape is sufficient to explain the observed diminishing returns and increasing costs, we simulated a series of 16 fitness landscapes with $n = 16$ binary sites, under the n -order model of g . In the k th landscape in the series ($1 \leq k \leq 16$), we considered up to the k th order of interaction. That is, each term of effect from the first to the k th-order interaction is a random variable independently drawn from the standard normal distribution, whereas all other terms are set to 0. When k rises from 1 to 16, I_{id} increases from 0 to 0.69 (Fig. 2a), which is close to the theoretically predicted value (see Methods). In all simulated landscapes except the one with $I_{id} = 0$, most if not all mutations exhibit a negative Pearson's correlation between fitness effect and background fitness (boxes in Fig. 2a). In addition, the larger the k and I_{id} , the more negative the correlations (boxes in Fig. 2a), supporting the role of idiosyncratic epistasis in creating the negative correlations. For comparison, 87.8% of mutations from the yeast tRNA fitness landscape show a negative correlation between fitness effect and background fitness (Fig. 2b). A similar trend is seen in other empirical phenotype landscapes (Extended Data Fig. 2a,b). Separating mutations that are beneficial or detrimental on the wild-type background or an arbitrary background reveals the familiar patterns of diminishing returns and increasing costs in both the simulated and empirical landscapes (Extended Data Fig. 3).

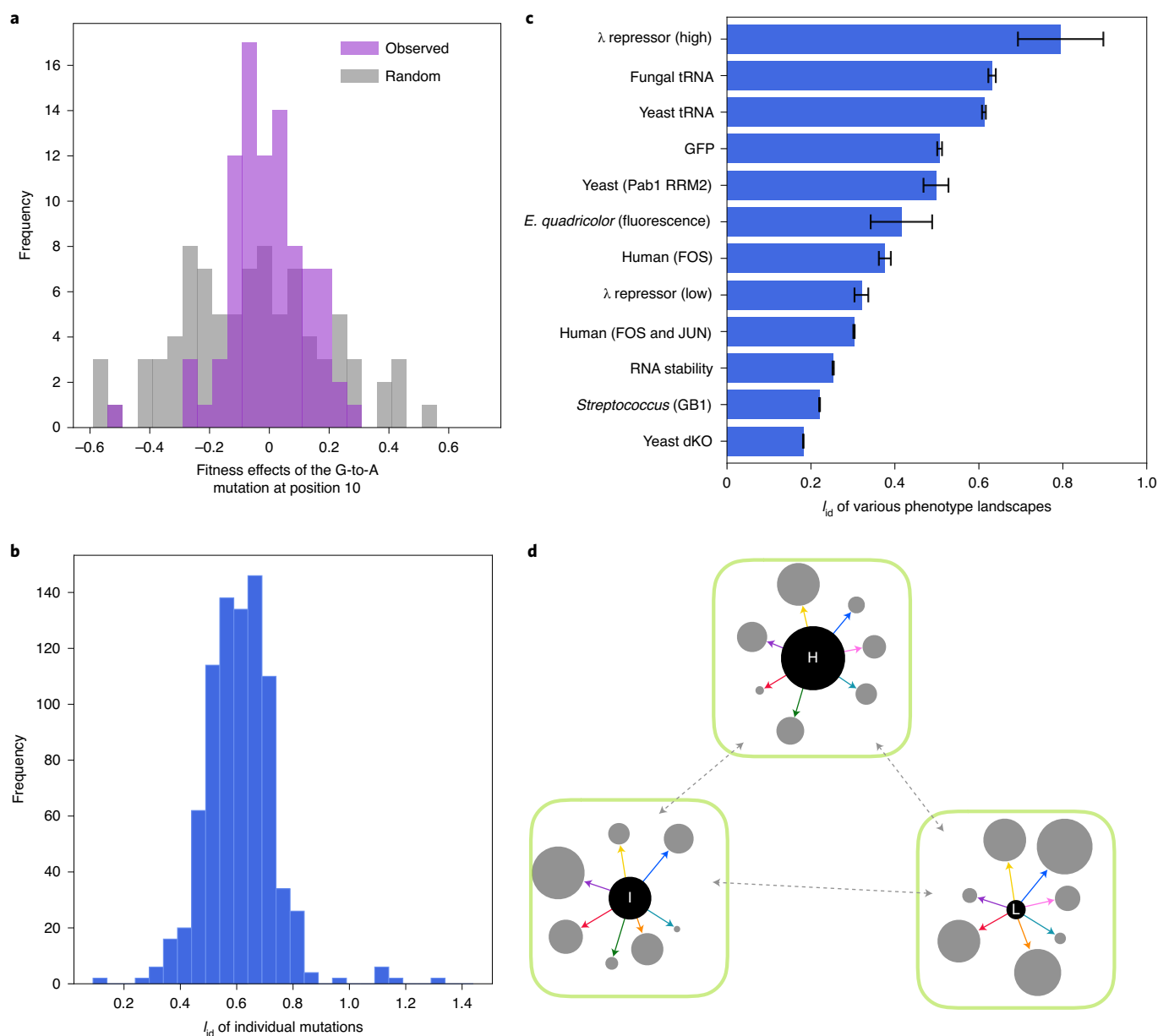


Fig. 1 | Idiosyncratic index of a wide variety of phenotype landscapes. **a**, Frequency distribution of the fitness effects of the mutation from G to A at position 10 across all available genetic backgrounds (purple) and the corresponding distribution of the fitness difference between two random genotypes for the same number of genotype pairs (grey) in the yeast tRNA fitness landscape. **b**, Frequency distribution of the s.d.-based idiosyncrasy index (I_{id}), which is the ratio of the s.d. of fitness effects of a particular mutation on different backgrounds to the s.d. of fitness differences between random genotype pairs, for all individual mutations in the yeast tRNA landscape. **c**, s.d.-based I_{id} values of various phenotype landscapes. Error bars show s.e.m. Detailed information on each landscape is provided in Supplementary Table 1. **d**, Schematic of a highly idiosyncratic fitness landscape. Genotypes are represented by circles, and the fitness of a genotype is represented by circle size. The three black circles labelled with H, I and L, respectively, indicate three focal genotypes with relatively high, intermediate and low fitness values. The grey circles represent one-mutation neighbours of the focal genotypes. Each light green outlined area encompasses a focal genotype and some one-mutation neighbours. Solid arrows indicate single mutations, whereas dotted arrows indicate multiple mutations. Solid arrows of the same colour indicate the same mutation. dKO, double knockout.

Furthermore, the effects of different mutations also negatively correlate with background fitness in the simulated landscapes (green diamonds in Fig. 2a; see Methods), as well as in the tRNA fitness landscape (Fig. 2c) and other empirical phenotype landscapes (Extended Data Fig. 2c,d). As mentioned, the negative correlation in the simulated landscape with $I_{id}=0$ (leftmost green diamond in Fig. 2a) is due to the contribution from the among-site and among-state variation in the additive effect; in the absence of this variation, all genotypes are equally fit, so the correlation disappears.

Idiosyncratic epistasis causes slowing fitness decreases in mutation accumulation. When random mutations accrue in a relatively fit population in the near absence of selection, population fitness is expected to decline. Because idiosyncratic epistasis renders random mutations on average less deleterious on relatively unfit genotypes than on relatively fit genotypes, the fitness decrease of the population is expected to decelerate during mutation accumulation until it reaches the mean fitness of all genotypes in the landscape, around which the fitness should subsequently fluctuate. We confirmed this

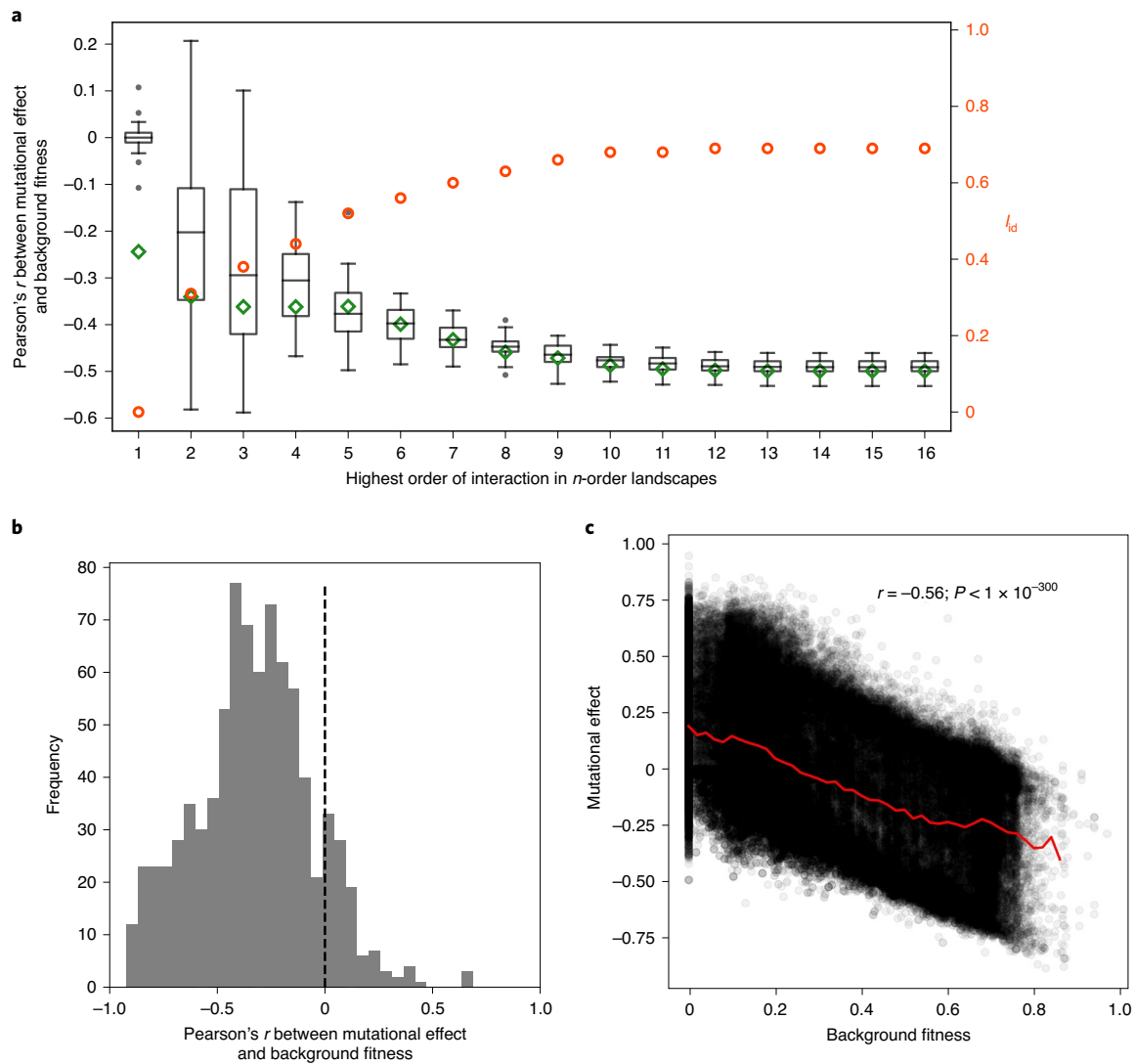


Fig. 2 | Negative correlation between mutational effect and background fitness as a result of idiosyncratic epistasis. a, Boxplot showing the distribution of Pearson's correlation coefficient (r) between mutational effect and background fitness for individual mutations in a series of n -order landscapes. The lower and upper edges of a box represent the first and third quartiles, respectively; the horizontal line inside the box indicates the median; the whiskers extend to the most extreme values inside inner fences (median ± 1.5 (third quartile – first quartile)); and the grey dots represent values outside the inner fences (outliers). Green diamonds represent r values for all mutations pooled in each landscape, while red circles indicate s.d.-based I_{id} values of the landscapes. **b**, Distribution of r for 828 individual mutations in the tRNA fitness landscape. **c**, Relationship between background fitness and mutational effect for 414 mutations (reversions not considered) in the tRNA fitness landscape. The red line depicts the running mean in non-overlapping x axis bins of width = 0.02, in all bins with more than ten data points. To avoid a spurious correlation due to shared measurement error on the x and y axis, we used three replicates of background fitness measures for the x axis and three other replicates for the y axis in **b** and **c**. For each mutation and its reversion, a randomly picked one is considered in **c**.

prediction in the simulated n -order landscapes. As k and I_{id} increase, the slowing curvature becomes more prominent (Fig. 3a). A change in mutational supply explains why the fitness decline is decelerating even when $I_{id} = 0$ (see Methods), and as expected this trend diminishes as n rises (Extended Data Fig. 4). For comparison, decelerating fitness declines are apparent during simulated mutation accumulations in the tRNA fitness landscape (Fig. 3b) and other empirical phenotype landscapes (Extended Data Fig. 5).

The decrease in fitness to the mean of all genotypes during mutation accumulation is observed in the n -order landscapes (Fig. 3a) and RNA stability landscape (Extended Data Fig. 5b), while the average mutation accumulation trajectory in tRNA (Fig. 3b) and green fluorescent protein (GFP) (Extended Data Fig. 5a) landscapes fluctuates above the mean of all genotypes. This latter phenomenon

is due to preferential sampling of genotypes close to the wild-type in the experimental data, trapping many simulated mutation accumulation trajectories around the wild-type. The former two theoretically simulated/calculated landscapes do not have such biases.

Idiosyncratic epistasis causes slowing fitness gains in adaptation.

Idiosyncratic epistasis, in combination with certain distributions of genotype fitness or interactive effects, creates the phenomenon of decelerating fitness gains during adaptation. In a solely additive landscape with $I_{id} = 0$, each adaptive trajectory is basically a random ordering of the beneficial mutations. Thus, the mean fitness increase of every step is the mean of the effect of all beneficial mutations, leading to a linear average trajectory regardless of the fitness distribution (Fig. 4a). In an idiosyncratic landscape with $I_{id} > 0$, the

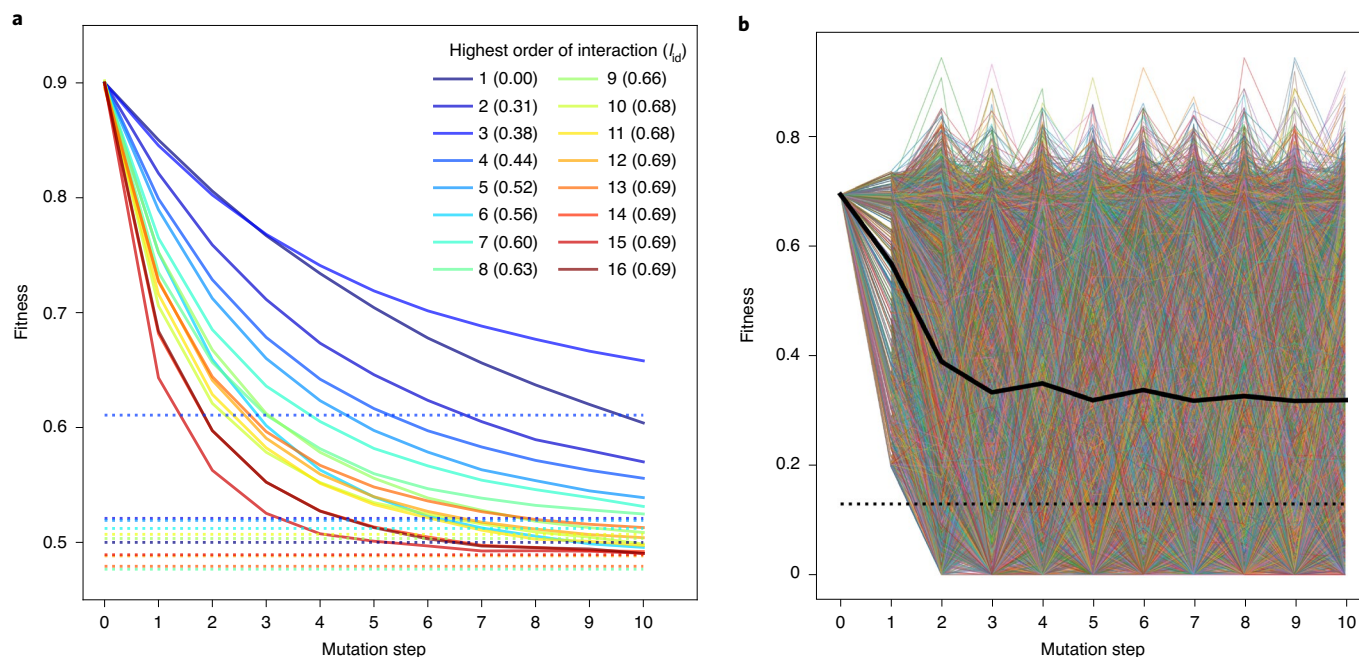


Fig. 3 | Fitness declines decelerate during mutation accumulation as a result of idiosyncratic epistasis. a, Average fitness trajectories simulated in a series of n -order landscapes. **b**, Ten thousand fitness trajectories of mutation accumulation simulated in the tRNA fitness landscape, with the average fitness of all trajectories at each step shown in black. Dotted lines indicate the mean fitness of all genotypes in the corresponding landscape.

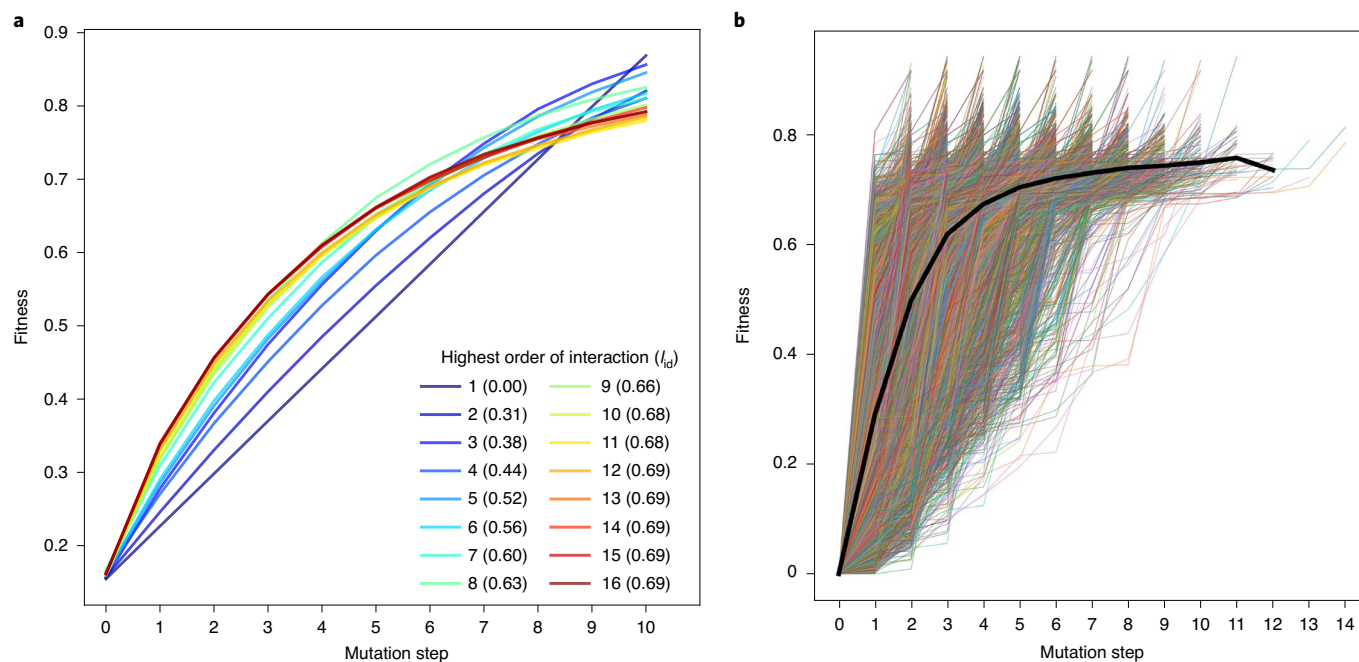


Fig. 4 | Adaptation slows as a result of idiosyncratic epistasis. a, Average adaptive trajectories simulated in a series of n -order landscapes. **b**, A total of 15,878 adaptive trajectories simulated in the tRNA fitness landscape, with the average fitness of all trajectories shown in black, at each step when the trajectory number exceeds 10.

mutation fixed at each step during adaptation is a random draw from beneficial mutations instead of all mutations. Because of this bias, the shape of the adaptive trajectory, unlike that of mutation accumulation, is dependent on the distribution of genotype fitness or interactive effects. For example, in a house-of-cards model (a special case of n -order landscapes with only the highest-order

interaction term), when the fitness of all genotypes is gamma distributed with a shape parameter of >1 , $=1$ or <1 (Extended Data Fig. 6a), fitness rises sublinearly, linearly or superlinearly with the number of mutations accumulated, respectively (Extended Data Fig. 6b) (see also ref. ³⁴). Although not sufficient for creating a decelerating adaptive trajectory, idiosyncrasy causes a decelerating

trajectory in a wide range of full n -order landscapes, including, for example, those with normal- (Fig. 4a), gamma- (Extended Data Fig. 6c) and beta-distributed (Extended Data Fig. 6d) interaction effects. As expected, adaptation slows more drastically with greater I_{id} (Fig. 4a and Extended Data Fig. 6c,d). Simulated adaptation also decelerates in the tRNA fitness landscape (Fig. 4b), as well as in other empirical phenotype landscapes (Extended Data Fig. 7), suggesting that the empirical cases fulfil both the idiosyncrasy and fitness distribution requirements.

Discussion

In summary, we proposed a simple theory that uses the idiosyncrasy of epistasis to explain some of the most commonly observed patterns of mutational effects and evolutionary trajectories. Phenotype landscapes of a variety of genes and taxa confirm our assumption of idiosyncratic epistasis. In contrast with common intuition, our work shows that diminishing returns and decelerating adaptations do not suggest a bias towards negative epistasis in the underlying fitness landscape or a concave landscape. Similarly, increasing costs and slowing fitness declines during mutation accumulation do not indicate a bias towards positive epistasis or a convex landscape. Thus, our theory resolves the uphill–downhill paradox.

Although the idiosyncrasy of epistasis is a major characteristic of empirical phenotype landscapes (Fig. 1c), biological interactions are not completely idiosyncratic. Rather, idiosyncratic epistasis should serve as a null model for the role of epistasis in mutational effects and evolution. For example, the relationship between the mutational robustness of a genotype (that is, fitness insensitivity to mutation) and its adaptability/evolvability to environmental challenges is debated^{35–37}. Our theory reveals an intrinsic positive correlation between robustness and adaptability due to idiosyncratic epistasis, because, as the fitness of a genotype rises, deleterious mutations are more detrimental (that is, there is lower robustness) and advantageous mutations are less beneficial (that is, there is lower adaptability). Deviations from this null expectation may reveal interesting forms of epistasis beyond idiosyncrasy. Similarly, because slowing fitness decreases during mutation accumulation naturally emerge from idiosyncratic epistasis, such observations need not be explained by selection for “genomic buffering against the fitness reduction caused by accumulated mutations”¹³. Rather, when this trend is absent or when the opposite trend is observed, selection for mutational robustness of the wild-type may be invoked³⁸.

A major question is the relative contributions of idiosyncrasy and various biological mechanisms to the universal uphill/downhill observations in empirical data. Clonal interference³⁹ and changes in mutational supply⁴⁰ probably contribute to slowing adaptation. Interestingly, diminishing returns contribute more greatly than changes of mutational supply to slowing adaptation even in a constant environment⁴¹, implying the importance of idiosyncrasy. Comparing adaptations of sexually and asexually reproducing organisms may provide a way to test the relative importance of clonal interference and idiosyncrasy. We emphasize that the high yet incomplete idiosyncrasy we find means that there is room for the action of various biological mechanisms. For example, the arrangement of enzymes in a metabolic pathway obviously has effects on the epistasis of mutations of enzyme genes²¹, and biological systems do show modularity⁴². It will be important to develop the idiosyncratic epistasis theory into a model that can be fit to empirical data and compared directly with other models. Given that the idiosyncratic epistasis theory makes only one assumption (that is, epistasis is at least somewhat idiosyncratic), such work will probably be fruitful in illuminating the causes and consequences of epistasis in a wide variety of systems.

How does the idiosyncrasy of epistasis arise from the underlying deterministic biological interactions? The n -order model reveals that the number of interactive terms determining the phenotype

of a genotype is potentially astronomical and that the same mutation differentially alters a substantial fraction of these terms in even slightly different genotypes. Consequently, it is difficult to predict the mutational effect in any particular genotype despite the underlying deterministic biological interactions, much like the apparently random outcome of a die roll that is deterministically shaped by myriad factors such as the movement of air molecules. That the universal trends of mutational effects and evolutionary trajectories emerge from this randomness due to idiosyncratic epistasis is no more surprising than the tendency of observing a smaller number in a second roll of a die when the first roll yields a five.

Methods

Number of terms of phenotypic effects altered by a mutation. Let g be the Malthusian fitness (fitness for short) of a genotype in an environment and let n be the number of nucleotide sites in a genome that are relevant to g . Here, g equals the sum of the additive fitness effect of every site (that is, the first-order interaction), the interactive effect of every pair of sites (that is, the second-order interaction), the interactive effect of every triplet of sites (that is, the third-order interaction), and so on. That is, g contains $\binom{n}{k}$ terms of effects of the k th order of interaction ($1 \leq k \leq n$), for a total of $2^n - 1$ terms. Among these terms, 2^{n-1} terms involve any particular site. Thus, a mutation at a single site potentially changes $2^{n-1}/(2^n - 1) \approx 50\%$ of all terms making up g .

Differentially altered terms of effects in two genotypes caused by the same mutation. When the same mutation of allele P changing to Q at site k occurs in two different genotypes that differ at m sites (k is not one of the m sites), the differentially altered terms of effects in these genotypes must involve site k and at least one of the m sites, and may also involve site(s) identical between the two genotypes. The total number of differentially altered terms equals the number of terms involving k and other site(s) that may or may not be identical between the two genotypes, minus the number of terms involving k and other site(s) that are identical between the two genotypes. The resulting number is $(2^{n-1} - 1) - (2^{n-m-1} - 1) = (2^m - 1)2^{n-m-1}$. When $m = 1$, the above number is 2^{n-2} . That is, up to $2^{n-2}/(2^n - 1) \approx 25\%$ of terms are differentially altered by the same mutation in two genotypes that differ at only one site. When $m = n - 1$, the above number is $2^{n-1} - 1$. That is, up to $(2^{n-1} - 1)/(2^n - 1) \approx 50\%$ of terms are differentially altered by the same mutation in two maximally different genotypes.

The fitness effect of a given mutation is negatively correlated with background fitness. Let us consider the n -order landscape model and focus on the mutation from the P allele to the Q allele at site k of the genome. We examine the fitness effect of this mutation on different genetic backgrounds. Let X represent any genotype with the P allele at site k . Among them, x_i is the i th genotype whose Malthusian fitness is R_{x_i} . R_{x_i} can be written as $R_{x_i} = A_{x_i} + I_{x_i} + I'_{x_i}$, where A_{x_i} is the sum of additive (that is, first-order interactive) effects, I_{x_i} is the sum of the second- to n th-order interactive effects involving the focal site k , and I'_{x_i} is the sum of the second- to n th-order interactive effects that do not involve site k .

Similarly, let Y represent any genotype with the Q allele at site k . For each genotype x_i , we have a corresponding genotype y_i that is identical to x_i except that site k now has the Q allele. The fitness of y_i can be written as $R_{y_i} = A_{y_i} + I_{y_i} + I'_{y_i}$, where A_{y_i} is the sum of additive (that is, first-order interactive) effects, I_{y_i} is the sum of the second- to n th-order interactive effects involving site k , and I'_{y_i} is the sum of the second- to n th-order interactive effects that do not involve site k .

Note that the difference in the additive effect between alleles P and Q is a constant that is not influenced by sites other than k . That is, $A_{y_i} - A_{x_i} = C$. Therefore, we have:

$$\begin{aligned} \text{Cov}(A_Y, A_X) &= \frac{1}{N} \sum_{i=1}^N (A_{y_i} - E(A_Y))(A_{x_i} - E(A_X)) \\ &= \frac{1}{N} \sum_{i=1}^N (A_{x_i} + C - E(A_X + C))(A_{x_i} - E(A_X)) \\ &= \frac{1}{N} \sum_{i=1}^N (A_{x_i} - E(A_X))(A_{x_i} - E(A_X)) = \text{Var}(A_X) \end{aligned}$$

Here, N is the total number of pairs of (x_i, y_i) and equals 4^{n-1} for a genome with n sites each with four states, Cov stands for covariance and Var stands for variance.

Also note that, because x_i and y_i are the same except at site k , $I'_{x_i} = I'_{y_i}$. Let $\text{Cor}(I_X, I_Y)$ be the Pearson correlation between I_X and I_Y . We have:

$\text{Cor}(I_X, I_Y) = \text{Cov}(I_X, I_Y) / \sqrt{\text{Var}(I_X)\text{Var}(I_Y)} \leq 1$. Hence, $\text{Cov}(I_X, I_Y) \leq \sqrt{\text{Var}(I_X)\text{Var}(I_Y)}$. Under the reasonable assumption that the corresponding interactive terms of x_i and y_i are sampled from the same distribution, $\text{Var}(I_X)$ and $\text{Var}(I_Y)$ are expected to be equal. Hence, $\text{Cov}(I_X, I_Y) \leq \sqrt{\text{Var}(I_X)\text{Var}(I_X)} = \text{Var}(I_X)$. Thus, $\text{Cov}(I_X, I_Y) = \text{Var}(I_X)$ when

I_X and I_Y have a correlation of 1; otherwise, $\text{Cov}(I_X, I_Y) < \text{Var}(I_X)$. When epistasis is to some extent idiosyncratic, I_Y does not correlate perfectly with I_X , resulting in $\text{Cov}(I_X, I_Y) < \text{Var}(I_X)$.

Under the assumption of independence among the interactive terms of a genotype, we have $\text{Cov}(\text{mutational effect, fitness of the background genotype}) = \text{Cov}(R_Y - R_X, R_X) = \text{Cov}((A_Y - A_X) + (I_Y - I_X) + (I'_Y - I'_X), A_X + I_X + I'_X) = \text{Cov}(C, A_X) + \text{Cov}(I_X, I_Y) - \text{Var}(I_X) + \text{Cov}(0, I'_X) = \text{Cov}(I_X, I_Y) - \text{Var}(I_X) < 0$. This mathematical result means that, when epistasis is to some extent idiosyncratic, for any given mutation, we expect a negative correlation between the background fitness and mutational effect, which is exactly what diminishing returns of beneficial mutations and increasing costs of deleterious mutations are. The above result holds when fitness is replaced with any phenotypic trait, as long as the trait value of each genotype can be expressed as the sum of the $2^n - 1$ terms of effects.

Mutational effect is generally negatively correlated with background fitness.

Below, we show that the preceding result about a given mutation also applies to different mutations. That is, we expect a negative correlation between the mutational effect and background fitness even when different mutations are considered. R_t , the Malthusian fitness of genotype t , can be expressed by $R_t = I^1_t + I^2_t + \dots + I^n_t + I^{1,2}_t + I^{1,3}_t + \dots + I^{n-1,n}_t + \dots + I^{1,2,\dots,n}_t$. Here, the superscript indicates the site(s) involved in an additive or interactive term. For instance, I^2_t stands for the additive effect of site 2 and $I^{1,2}_t$ stands for the interactive effect between sites 1 and 2.

Let X represent an arbitrary genotype and Y represent another genotype that differs from X by a particular mutation named W that occurs at site k . We have:

$$R_X = I^1_X + I^2_X + \dots + I^n_X + I^{1,2}_X + I^{1,3}_X + \dots + I^{n-1,n}_X + \dots + I^{1,2,\dots,n}_X \text{ and}$$

$$R_Y = I^1_Y + I^2_Y + \dots + I^n_Y + I^{1,2}_Y + I^{1,3}_Y + \dots + I^{n-1,n}_Y + \dots + I^{1,2,\dots,n}_Y.$$

In the above, all corresponding terms between I_X and I_Y are equal except for the terms involving k . So,

$$R_Y - R_X = (I^k_Y - I^k_X) + (I^{1,k}_Y - I^{1,k}_X) + \dots + (I^{n,k}_Y - I^{n,k}_X) + \dots + (I^{1,2,\dots,n,k}_Y - I^{1,2,\dots,n,k}_X).$$

Under the assumption that all I terms in an R are independent of one another, $\text{Cov}(\text{mutational effect, background fitness}) = \text{Cov}(R_Y - R_X, R_X) =$

$$\text{Cov}(I^k_Y - I^k_X, I^k_X) + \text{Cov}(I^{1,k}_Y - I^{1,k}_X, I^k_X) + \dots + \text{Cov}(I^{n,k}_Y - I^{n,k}_X, I^k_X) + \dots + \text{Cov}(I^{1,2,\dots,n,k}_Y - I^{1,2,\dots,n,k}_X, I^{1,2,\dots,n,k}_X).$$

According to the law of total variance and the law of total covariance, we can expand each term in the above equation. Let us use the second-order interaction between site s and site k as an example.

$$\begin{aligned} \text{Cov}(I^{s,k}_Y - I^{s,k}_X, I^{s,k}_X) &= \text{Cov}(I^{s,k}_Y, I^{s,k}_X) - \text{Var}(I^{s,k}_X) = \\ &E(\text{Cov}(I^{s,k}_Y, I^{s,k}_X|W)) + \text{Cov}(E(I^{s,k}_Y|W), E(I^{s,k}_X|W)) - E(\text{Var}(I^{s,k}_X|W)) \\ &\quad - \text{Var}(E(I^{s,k}_X|W)) \\ &= E(\text{Cov}(I^{s,k}_Y, I^{s,k}_X|W) - \text{Var}(I^{s,k}_X|W)) + \text{Cov}(E(I^{s,k}_Y - I^{s,k}_X|W), E(I^{s,k}_X|W)). \end{aligned}$$

As shown in the section about a given mutation, as long as there is some degree of idiosyncrasy, $\text{Cov}(I^{s,k}_Y, I^{s,k}_X|W) < \text{Var}(I^{s,k}_X|W)$.

So, $E(\text{Cov}(I^{s,k}_Y, I^{s,k}_X|W) - \text{Var}(I^{s,k}_X|W)) < 0$. Furthermore, $\text{Cov}(E(I^{s,k}_Y - I^{s,k}_X|W), E(I^{s,k}_X|W)) = 0$, because $E(I^{s,k}_Y - I^{s,k}_X|W) = 0$ under the reasonable assumption that, given W , $I^{s,k}_X$ and $I^{s,k}_Y$ follow the same distribution. Hence, $\text{Cov}(I^{s,k}_Y - I^{s,k}_X, I^{s,k}_X) < 0$. The same conclusion applies to all terms except the first-order interactive (additive) term, which is

$$\begin{aligned} \text{Cov}(I^k_Y - I^k_X, I^k_X) &= E(\text{Cov}(I^k_Y, I^k_X|W) - \text{Var}(I^k_X|W)) \\ &\quad + \text{Cov}(E(I^k_Y - I^k_X|W), E(I^k_X|W)). \end{aligned}$$

Because additive effects are independent of the genetic background, given W , I^k_Y and I^k_X are both fixed and are two randomly sampled values from the same distribution. Hence, $\text{Cov}(I^k_Y, I^k_X|W) = 0$ and $\text{Var}(I^k_X|W) = 0$. So, $E(\text{Cov}(I^k_Y, I^k_X|W) - \text{Var}(I^k_X|W)) = 0$. $E(I^k_Y|W) = I^k_Y|W$ and $E(I^k_X|W) = I^k_X|W$. As W varies, $I^k_Y|W$ and $I^k_X|W$ are two random variables from the same distribution. They have the same variance and are not usually completely correlated. So,

$$\begin{aligned} \text{Cov}(E(I^k_Y - I^k_X|W), E(I^k_X|W)) &= \text{Cov}(I^k_Y - I^k_X|W, I^k_X|W) \\ &= \text{Cov}(I^k_Y, I^k_X|W) - \text{Var}(I^k_X|W) < 0. \end{aligned}$$

Under the special case when all additive terms are equal,

$$\text{Cov}(E(I^k_Y - I^k_X|W), E(I^k_X|W)) = 0.$$

Thus, $\text{Cov}(\text{mutational effect, background fitness}) =$

$$\begin{aligned} &E(\text{Cov}(I^k_Y, I^k_X|W) - \text{Var}(I^k_X|W)) + \text{Cov}(E(I^k_Y - I^k_X|W), E(I^k_X|W)) + \\ &E(\text{Cov}(I^{1,k}_Y, I^{1,k}_X|W) - \text{Var}(I^{1,k}_X|W)) + \text{Cov}(E(I^{1,k}_Y - I^{1,k}_X|W), E(I^{1,k}_X|W)) + \\ &\dots + E(\text{Cov}(I^{n,k}_Y, I^{n,k}_X|W) - \text{Var}(I^{n,k}_X|W)) + \text{Cov}(E(I^{n,k}_Y - I^{n,k}_X|W), E(I^{n,k}_X|W)) \\ &+ \dots + E(\text{Cov}(I^{1,2,\dots,n,k}_Y, I^{1,2,\dots,n,k}_X|W) - \text{Var}(I^{1,2,\dots,n,k}_X|W)) + \\ &\text{Cov}(E(I^{1,2,\dots,n,k}_Y - I^{1,2,\dots,n,k}_X|W), E(I^{1,2,\dots,n,k}_X|W)) = \\ &\quad \text{Cov}(I^k_Y - I^k_X|W, I^k_X|W) + E(\text{Cov}(I^{1,k}_Y, I^{1,k}_X|W) - \text{Var}(I^{1,k}_X|W)) \end{aligned}$$

$+ \dots + E(\text{Cov}(I^{n,k}_Y, I^{n,k}_X|W) - \text{Var}(I^{n,k}_X|W)) + \dots + E(\text{Cov}(I^{1,2,\dots,n,k}_Y, I^{1,2,\dots,n,k}_X|W) - \text{Var}(I^{1,2,\dots,n,k}_X|W)) < 0$. Therefore, in the n -order model, mutational effect is negatively correlated with background fitness even for different mutations. As shown in the above mathematical derivation, this negative correlation has two sources: unequal additive effects and idiosyncratic epistasis. Given the same additive effects, increasing the idiosyncrasy in epistasis strengthens the negative correlation. As in the preceding section, the result here applies to any phenotypic trait as long as the trait value of a genotype can be expressed as the sum of the $2^n - 1$ terms of effects.

Expected idiosyncrasy index under the n -order landscape model. The variance of the effect of a particular mutation across all genetic backgrounds can be calculated as follows. Let X represent an arbitrary genotype and Y represent another genotype that differs from X at site k only. We have shown earlier that:

$$R_X = I^1_X + I^2_X + \dots + I^n_X + I^{1,2}_X + I^{1,3}_X + \dots + I^{n-1,n}_X + \dots + I^{1,2,\dots,n}_X \text{ and}$$

$$R_Y = I^1_Y + I^2_Y + \dots + I^n_Y + I^{1,2}_Y + I^{1,3}_Y + \dots + I^{n-1,n}_Y + \dots + I^{1,2,\dots,n}_Y.$$

In the above, all corresponding terms between I_X and I_Y are equal except for the terms involving k . So,

$$R_Y - R_X = (I^k_Y - I^k_X) + (I^{1,k}_Y - I^{1,k}_X) + \dots + (I^{n,k}_Y - I^{n,k}_X) + \dots + (I^{1,2,\dots,n,k}_Y - I^{1,2,\dots,n,k}_X)$$

and $\text{Var}(R_Y - R_X) = \text{Var}(I^k_Y - I^k_X) + \text{Var}(I^{1,k}_Y - I^{1,k}_X) + \dots +$

$\text{Var}(I^{n,k}_Y - I^{n,k}_X) + \dots + \text{Var}(I^{1,2,\dots,n,k}_Y - I^{1,2,\dots,n,k}_X)$. If we assume that all interactive terms for X and Y are independent with the same variance σ^2 , $\text{Var}(R_Y - R_X) = 2^n \sigma^2$.

If there are M states at each site, among the k th-order interactive terms, $\binom{n}{k} (1/M)^k$ terms are expected to be the same between two random genotypes. One can show that $\sum_{k=1}^n \binom{n}{k} (1/M)^k = \sum_{k=1}^n \frac{n!}{k!(n-k)!} \cdot (1/M)^k \approx \sum_{k=1}^n \frac{n!}{k!} \cdot (1/M)^k \approx e^{n/M}$.

Thus, two random genotypes are expected to differ by approximately $2^n - 1 - e^{n/M}$ terms. Hence, the variance of the fitness difference between two random genotypes is $\text{Var}(R_Y - R_X) = 2(2^n - 1 - e^{n/M})\sigma^2$. Because $M \geq 2$, $e^{n/M} < 2^n$. So, when n is large, $\text{Var}(R_Y - R_X)$ is approximately $2^{n+1}\sigma^2$. Therefore, the idiosyncrasy index becomes $\frac{\sqrt{2^n \sigma^2}}{\sqrt{2^{n+1} \sigma^2}} = \frac{1}{\sqrt{2}} = 0.71$. Our numerical finding (the most right red dot in Fig. 2a) confirms this result.

Mutational supply and evolutionary trajectories. During adaptation, if the supply of beneficial mutations diminishes as the fitness of a population rises, the speed of population fitness increase per unit of time will decline. However, if the speed of fitness increase is measured per beneficial mutation accrued as in the present study, the reducing supply of beneficial mutations will not reduce the speed of fitness increase.

During mutation accumulation in the near absence of selection, as the population fitness declines, the supply of beneficial mutations should increase and the supply of deleterious mutations should decrease. Thus, even under a purely additive model, the speed of population fitness decrease slows. However, when only the first few mutations accrued are examined, this phenomenon of slowing fitness decreases should be minimal under the purely additive model unless the number of possible mutations is very limited.

Empirical phenotype landscapes. An unbiased search for phenotype landscape data published between 2000 and 2019 was performed using Google Scholar with

words such as “epistasis”, “fitness landscape” or “genetic interaction”. A total of 18 datasets were found for which quantitative phenotype values were published or could be calculated without extensive analysis (for example, studies reporting only sequencing reads were excluded) and which included genotypes with at least two mutations compared with the reference genotype. Measured phenotypes included protein function, such as log[fluorescence], log[Wrightian fitness] or growth rate, and colony size. For landscapes reporting genotypes with nucleotide mutations, all 12 classes of single mutations were considered. For landscapes reporting genotypes with amino acid mutations, all 380 mutations between any two amino acids were considered as single mutations. Genotypes with fitness at the minimum detection limit (for example, non-fluorescent GFP genotypes) or that were lethal or non-growing (for example, tRNA genotypes with Wrightian fitness relative to the wild-type = 0.5) were excluded. A final set of 12 studies with at least ten single mutations and at least an average of ten fitness effects measured per mutation were used for further analysis. Supplementary Table 1 lists the basic information of these phenotype landscapes. The original study of the tRNA fitness landscape reported Wrightian fitness relative to the wild-type; we computed Malthusian fitness = $\log[\text{Wrightian fitness}]$ in the present study.

To investigate the evolution of an arbitrary RNA that has a complex phenotype with no measurement error, we mapped the RNA stability landscape of RNAs of 72 nucleotides. Similar to ref. ³⁶, we defined the fitness of a sequence as the absolute value of the minimum free energy of its most stable secondary structure, calculated using ViennaRNA (<https://www.tbi.univie.ac.at/RNA/>). The starting sequence was taken from a yeast tRNA sequence. Mutants were randomly created on each of two million random background genotypes, and this set of genotypes was used for subsequent analyses.

Simulating idiosyncratic fitness landscapes. We simulated a series of 16-site fitness landscapes under n -order models with two states (A/T) per site, including all 65,536 genotypes. The fitness of a genotype is determined by additive effects (referred to as first-order interactions) and interactive effects. For the k th-order interaction ($1 \leq k \leq 16$), there are $\frac{16!}{(16-k)!k!}$ interactive terms. For each of these terms, there are 2^k possible state combinations. The fitness effect of each state combination of each interaction term for each order of interaction is drawn independently from the standard normal distribution, and the fitness of the genotype concerned is the sum of all of these terms. Sixteen landscapes were made by including successively increasing orders of interactions. For instance, the first landscape contains only first-order interactions (purely additive); the second landscape contains only first- and second-order interactions; and the sixteenth landscape contains all orders of interactions. In each landscape, fitness values are linearly scaled to the interval of [0, 1]. As expected, I_{id} increased with the number of orders of interactions included (orange circles in Fig. 2a), because the numerator in the formula of I_{id} increased whereas the denominator stayed more or less constant. In each of these landscapes, epistasis between mutations is symmetrically distributed, with the mean equal to 0. We also simulated additive landscapes with larger n values to examine the linearity of fitness decreases during mutation accumulation.

Estimating the idiosyncrasy index. For each single mutation in a fitness landscape, we calculated its fitness effects on all genetic backgrounds available. For each mutation, we also derived a control set of fitness effects by randomly sampling (with replacement) the same number of pairs of genotypes from the landscape as used for the mutation and computing the fitness difference for each pair. We then calculated the s.d. of fitness effects and range of fitness effects for each mutation and its control dataset. For each mutation, we calculated the ratio in the s.d. (or range) between the actual data and the control data. The average ratio across all single mutations is the I_{id} of the landscape, and the error bars in Fig. 1c are the s.e.m. The same method is used to estimate I_{id} of other phenotype landscapes. Although empirical phenotype landscape data typically include only a small fraction of non-randomly sampled genotypes and their phenotypes, this non-random sampling is not expected to substantially affect I_{id} estimation, because both the variation of the effect of a mutation and the variation in the control data are estimated using the available landscape data. The theoretical minimum and maximum I_{id} for an individual mutation are, asymptotically, 0 and 1, respectively. However, because we use randomly sampled mutations to empirically estimate I_{id} , the value of I_{id} may be above 1 in some cases.

If a mutation's range of effects in different backgrounds crosses 0, the mutation exhibits sign epistasis. For each landscape, we calculated the proportion of mutations that exhibited sign epistasis, excluding mutations with little reported information (that is, those that appeared on fewer than five backgrounds).

Examining the correlation between background fitness and mutational effect. For the simulated n -order landscapes and empirical landscapes (tRNA fitness, GFP activity and RNA stability), Pearson's correlation coefficient was calculated between the mutational effect on a particular trait and the background trait value for each single mutation. Mutations appearing on fewer than four backgrounds were excluded. Pearson's correlation coefficient was also calculated between all mutational effects and background trait values for each landscape.

In the tRNA fitness landscape, the fitness of each genotype was measured in six replicates. To exclude artificial correlation due to measurement error, the

background fitness of each case of a single mutation was calculated using the mean fitness value from replicates 1–3, while the mutational effect was computed using mean fitness from replicates 4–6.

Additionally, two mutations that are the reverse of each other on the same background can automatically create a negative correlation between all mutational effects and background fitness. Hence, in each landscape where this could occur, we randomly chose a mutation or its reversion when pooling all mutations together (Fig. 2a (green diamonds), Fig. 2c and Extended Data Fig. 2c,d).

For analysis of diminishing returns and increasing costs, mutations were deemed beneficial or detrimental depending on their effect on the wild-type genotype in GFP and tRNA, or a random arbitrary genotype in RNA stability, or on a genotype with a fitness value closest to the average fitness in the n -order landscapes.

Simulating evolutionary trajectories in mutation accumulation. For each empirical landscape, mutation accumulation from an initial genotype was simulated by randomly choosing single mutations until the resulting genotype was non-functional (GFP), or for a maximum of ten mutational steps (tRNA) or 50 mutational steps (RNA stability). For all plots concerning mutation accumulation, the mean phenotype value of the landscape was calculated from all genotypes.

For the GFP landscape, genotypes were not allowed to be revisited within a trajectory. If a mutation accumulation trajectory was part of another simulated trajectory, the shorter trajectory was discarded. A total of 3,069 mutation accumulation trajectories were simulated from each of 3,069 initial genotypes with activity equal to or greater than that of the wild-type. In the tRNA fitness landscape, 10,000 mutation accumulation trajectories were simulated starting from the wild-type genotype. In the n -order fitness landscapes, 10,000 mutation accumulation trajectories were simulated starting from the genotype with fitness closest to the 90th percentile. For the RNA stability landscape, a total of 350 mutation accumulation trajectories were simulated starting with the final genotypes from the simulated adaptations.

Simulating adaptive trajectories. For each empirical landscape, adaptation from an initial genotype was simulated by randomly choosing a single beneficial mutation, which increased the value of the trait concerned, until no more single beneficial mutations were available. A total of 5,000 adaptive trajectories starting from 3,441 initial genotypes chosen from the bottom 15% of genotypes (activity ≤ -0.4) were simulated for the GFP landscape. A total of 350 adaptive trajectories starting from 350 initial genotypes chosen from the bottom 0.0175% of genotypes in the RNA stability landscape were simulated. In the tRNA fitness landscape, we simulated five adaptive trajectories starting from each genotype with fitness = 0.5; trajectories longer than two steps were retained, totalling 15,878 trajectories. In the n -order fitness landscapes, adaptations start from all genotypes in the bottom 20% of fitness distribution; among ten adaptation simulations starting from each genotype, trajectories equal to or longer than two steps were retained.

Reporting Summary. Further information on research design is available in the Nature Research Reporting Summary linked to this article.

Data availability

Data analysis and simulations for all landscapes except the tRNA and model landscapes were performed using R version 3.5.2. Analysis and simulations for the tRNA and model landscapes were performed using Python version 3.6.9. All figures were made with the matplotlib package in Python and Keynote. New data are available at <https://github.com/lyonsdm/ideosyncrasy>.

Code availability

Code is available at <https://github.com/lyonsdm/ideosyncrasy>.

Received: 15 February 2020; Accepted: 23 July 2020;
Published online: 7 September 2020

References

- Phillips, P. C. Epistasis—the essential role of gene interactions in the structure and evolution of genetic systems. *Nat. Rev. Genet.* **9**, 855–867 (2008).
- Kondrashov, A. S. Deleterious mutations and the evolution of sexual reproduction. *Nature* **336**, 435–440 (1988).
- Crow, J. F. & Kimura, M. Efficiency of truncation selection. *Proc. Natl Acad. Sci. USA* **76**, 396–399 (1979).
- Zhang, J. Epistasis analysis goes genome-wide. *PLoS Genet.* **13**, e1006558 (2017).
- Kemble, H., Nghe, P. & Tenaillon, O. Recent insights into the genotype–phenotype relationship from massively parallel genetic assays. *Evol. Appl.* **12**, 1721–1742 (2019).
- Couce, A. & Tenaillon, O. A. The rule of declining adaptability in microbial evolution experiments. *Front. Genet.* **6**, 99 (2015).

7. Barrick, J. E. et al. Genome evolution and adaptation in a long-term experiment with *Escherichia coli*. *Nature* **461**, 1243–1247 (2009).
8. MacLean, R., Perron, G. G. & Gardner, A. Diminishing returns from beneficial mutations and pervasive epistasis shape the fitness landscape for rifampicin resistance in *Pseudomonas aeruginosa*. *Genetics* **186**, 1345–1354 (2010).
9. Chou, H.-H., Chiu, H.-C., Delaney, N. F., Segrè, D. & Marx, C. J. Diminishing returns epistasis among beneficial mutations decelerates adaptation. *Science* **332**, 1190–1192 (2011).
10. Kryazhinskiy, S., Rice, D. P., Jerison, E. R. & Desai, M. M. Global epistasis makes adaptation predictable despite sequence-level stochasticity. *Science* **344**, 1519–1522 (2014).
11. Khan, A. I., Dinh, D. M., Schneider, D., Lenski, R. E. & Cooper, T. F. Negative epistasis between beneficial mutations in an evolving bacterial population. *Science* **332**, 1193–1196 (2011).
12. Miller, C. R. The treacheries of adaptation. *Science* **366**, 418–419 (2019).
13. Maisnier-Patin, S. et al. Genomic buffering mitigates the effects of deleterious mutations in bacteria. *Nat. Genet.* **37**, 1376–1379 (2005).
14. Perfeito, L., Sousa, A., Bataillon, T. & Gordo, I. Rates of fitness decline and rebound suggest pervasive epistasis. *Evolution* **68**, 150–162 (2014).
15. De la Iglesia, F. & Elena, S. F. Fitness declines in Tobacco etch virus upon serial bottleneck transfers. *J. Virol.* **81**, 4941–4947 (2007).
16. Johnson, M. S., Martsul, A., Kryazhinskiy, S. & Desai, M. M. Higher-fitness yeast genotypes are less robust to deleterious mutations. *Science* **366**, 490–493 (2019).
17. Wei, X. & Zhang, J. Patterns and mechanisms of diminishing returns from beneficial mutations. *Mol. Biol. Evol.* **36**, 1008–1021 (2019).
18. Sanjuan, R. & Elena, S. F. Epistasis correlates to genomic complexity. *Proc. Natl Acad. Sci. USA* **103**, 14402–14405 (2006).
19. Schoustra, S., Hwang, S., Krug, J. & de Visser, J. A. Diminishing-returns epistasis among random beneficial mutations in a multicellular fungus. *Proc. Biol. Sci.* **283**, 20161376 (2016).
20. Blanquart, F., Achaz, G., Bataillon, T. & Tenaillon, O. Properties of selected mutations and genotypic landscapes under Fisher's geometric model. *Evolution* **68**, 3537–3554 (2014).
21. He, X., Qian, W., Wang, Z., Li, Y. & Zhang, J. Prevalent positive epistasis in *Escherichia coli* and *Saccharomyces cerevisiae* metabolic networks. *Nat. Genet.* **42**, 272–276 (2010).
22. Draghi, J. A. & Plotkin, J. B. Selection biases the prevalence and type of epistasis along adaptive trajectories. *Evolution* **67**, 3120–3131 (2013).
23. Greene, D. & Crona, K. The changing geometry of a fitness landscape along an adaptive walk. *PLoS Comput. Biol.* **10**, e1003520 (2014).
24. Li, C., Qian, W., Maclean, M. & Zhang, J. The fitness landscape of a tRNA gene. *Science* **352**, 837–840 (2016).
25. Li, X., Lalic, J., Baeza-Centurion, P., Dhar, R. & Lehner, B. Changes in gene expression predictably shift and switch genetic interactions. *Nat. Commun.* **10**, 3886 (2019).
26. Domingo, J., Diss, G. & Lehner, B. Pairwise and higher-order genetic interactions during the evolution of a tRNA. *Nature* **558**, 117–121 (2018).
27. Sarkisyan, K. S. et al. Local fitness landscape of the green fluorescent protein. *Nature* **533**, 397–401 (2016).
28. Melamed, D., Young, D. L., Gamble, C. E., Miller, C. R. & Fields, S. Deep mutational scanning of an RRM domain of the *Saccharomyces cerevisiae* poly(A)-binding protein. *RNA* **19**, 1537–1551 (2013).
29. Poelwijk, F. J., Socolich, M. & Ranganathan, R. Learning the pattern of epistasis linking genotype and phenotype in a protein. *Nat. Commun.* **10**, 4213 (2019).
30. Diss, G. & Lehner, B. The genetic landscape of a physical interaction. *eLife* **7**, e32472 (2018).
31. Olson, C. A., Wu, N. C. & Sun, R. A comprehensive biophysical description of pairwise epistasis throughout an entire protein domain. *Curr. Biol.* **24**, 2643–2651 (2014).
32. Costanzo, M. et al. A global genetic interaction network maps a wiring diagram of cellular function. *Science* **353**, aaf1420 (2016).
33. De Visser, J. A. & Krug, J. Empirical fitness landscapes and the predictability of evolution. *Nat. Rev. Genet.* **15**, 480–490 (2014).
34. Seetharaman, S. & Jain, K. Adaptive walks and distribution of beneficial fitness effects. *Evolution* **68**, 965–975 (2014).
35. Masel, J. & Trotter, M. V. Robustness and evolvability. *Trends Genet.* **26**, 406–414 (2010).
36. Wagner, A. Robustness and evolvability: a paradox resolved. *Proc. Biol. Sci.* **275**, 91–100 (2008).
37. Wei, X. & Zhang, J. Why phenotype robustness promotes phenotype evolvability. *Genome Biol. Evol.* **9**, 3509–3515 (2017).
38. Bershtein, S., Segal, M., Bekerman, R., Tokuriki, N. & Tawfik, D. S. Robustness–epistasis link shapes the fitness landscape of a randomly drifting protein. *Nature* **444**, 929–932 (2006).
39. Gerrish, P. J. & Lenski, R. E. The fate of competing beneficial mutations in an asexual population. *Genetica* **102–103**, 127–144 (1998).
40. Silander, O. K., Tenaillon, O. & Chao, L. Understanding the evolutionary fate of finite populations: the dynamics of mutational effects. *PLoS Biol.* **5**, e94 (2007).
41. Wunsche, A. et al. Diminishing-returns epistasis decreases adaptability along an evolutionary trajectory. *Nat. Ecol. Evol.* **1**, 0061 (2017).
42. Wagner, G. P., Pavlicev, M. & Cheverud, J. M. The road to modularity. *Nat. Rev. Genet.* **8**, 921–931 (2007).

Acknowledgements

We thank A. Kondrashov, A. Lauring and members of the Zhang laboratory for valuable comments. This work was supported by US National Institutes of Health (NIH) research grant R01GM103232 to J.Z. D.M.L. was supported by NIH F31AI140618.

Author contributions

D.M.L., Z.Z. and J.Z. conceived of and designed the study. D.M.L. and Z.Z. performed the research and analysed the data. H.X. provided the mathematical proofs. All authors contributed to writing the paper.

Competing interests

The authors declare no competing interests.

Additional information

Extended data is available for this paper at <https://doi.org/10.1038/s41559-020-01286-y>.

Supplementary information is available for this paper at <https://doi.org/10.1038/s41559-020-01286-y>.

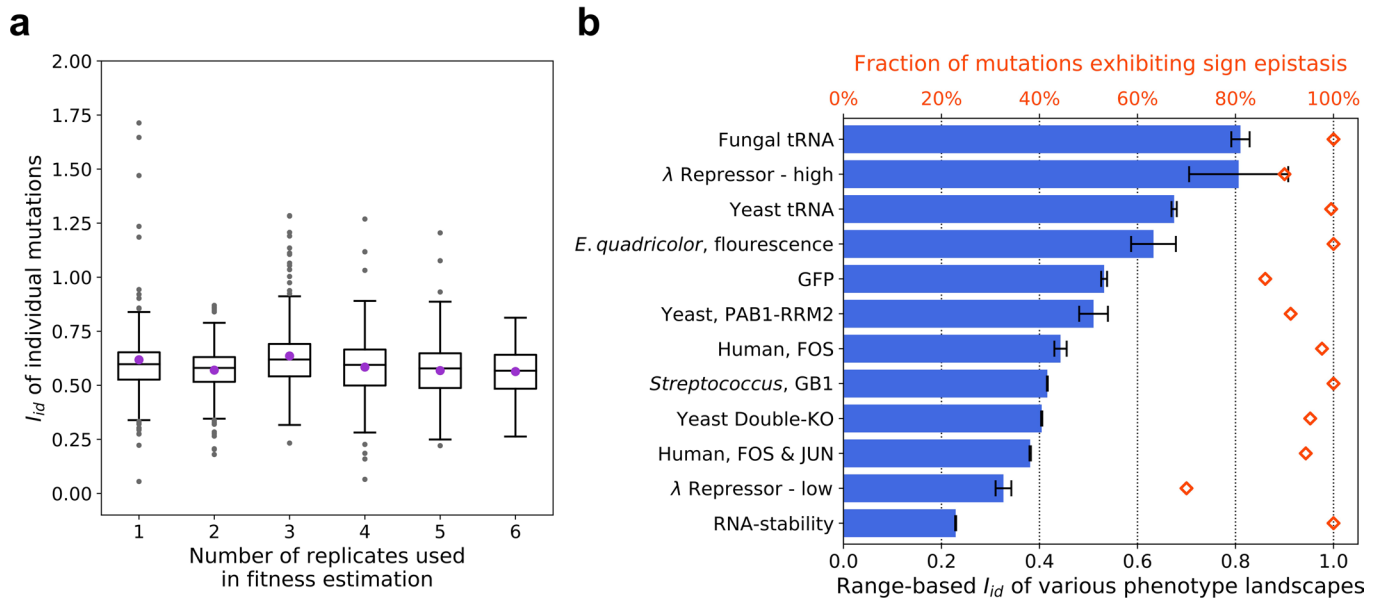
Correspondence and requests for materials should be addressed to J.Z.

Peer review information Peer reviewer reports are available.

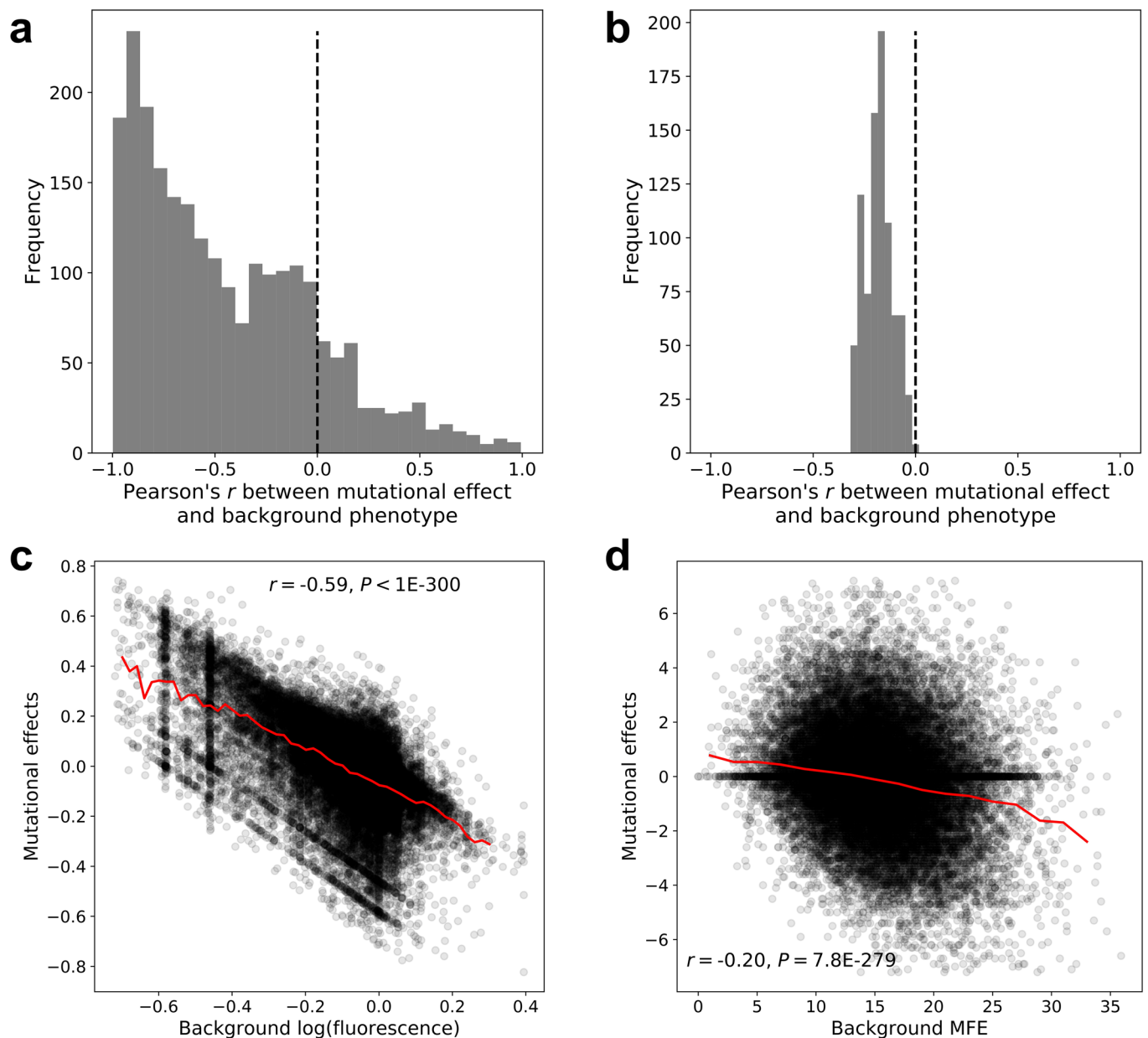
Reprints and permissions information is available at www.nature.com/reprints.

Publisher's note Springer Nature remains neutral with regard to jurisdictional claims in published maps and institutional affiliations.

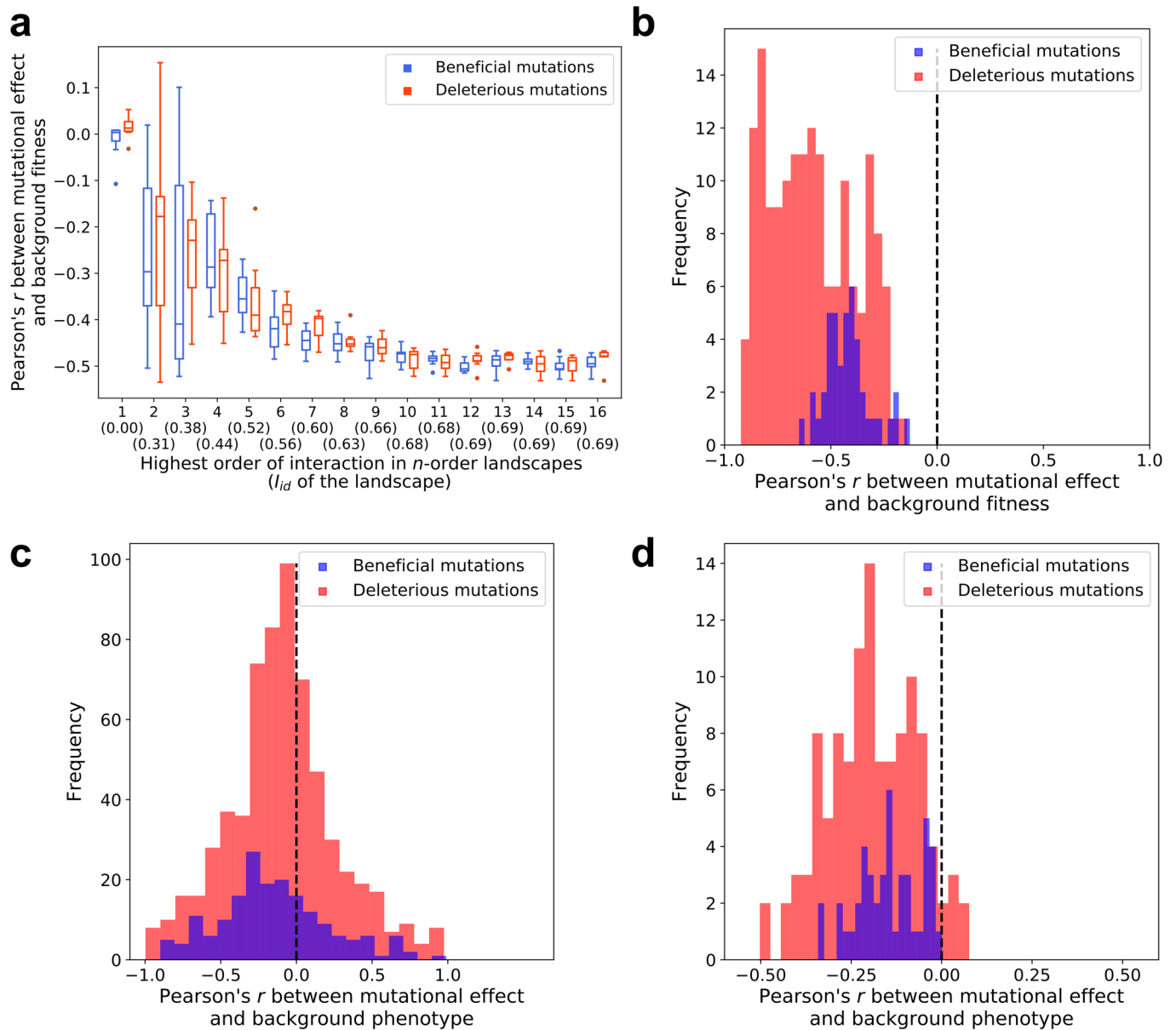
© The Author(s), under exclusive licence to Springer Nature Limited 2020



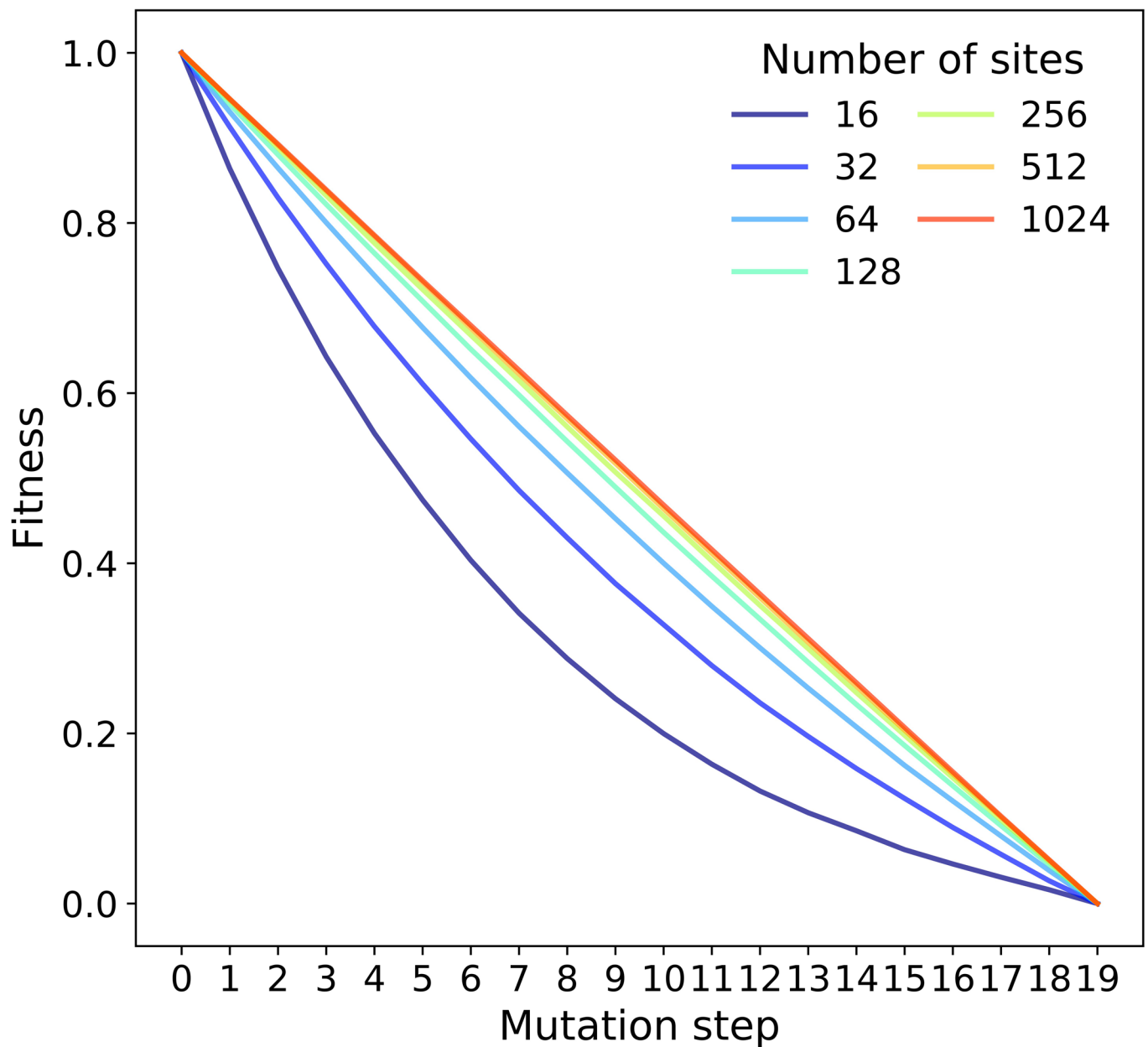
Extended Data Fig. 1 | The high idiosyncrasy indices (I_{id}) observed are not due to phenotype measurement errors or the use of standard deviation (SD) instead of range of mutational effects. **a, SD-based I_{id} of the yeast tRNA fitness landscape is insensitive to the number of experimental replicates used in the fitness estimation. Boxplots show the distribution of I_{id} values of 828 single mutations in the tRNA landscape, calculated based on different numbers of replicates. The lower and upper edges of a box represent the first (qu1) and third (qu3) quartiles, respectively, the horizontal line inside the box indicates the median (md), the whiskers extend to the most extreme values inside inner fences, $md \pm 1.5(qu3 - qu1)$, and the grey dots represent values outside the inner fences (outliers). Violet dots show mean I_{id} of all mutations calculated based on respective numbers of replicates. **b**, Range-based I_{id} for various phenotype landscapes. Error bars show standard errors. Detailed information of each landscape is provided in Supplementary Table 1. Shown in red is the fraction of mutations exhibiting sign epistasis in each phenotype landscape.**



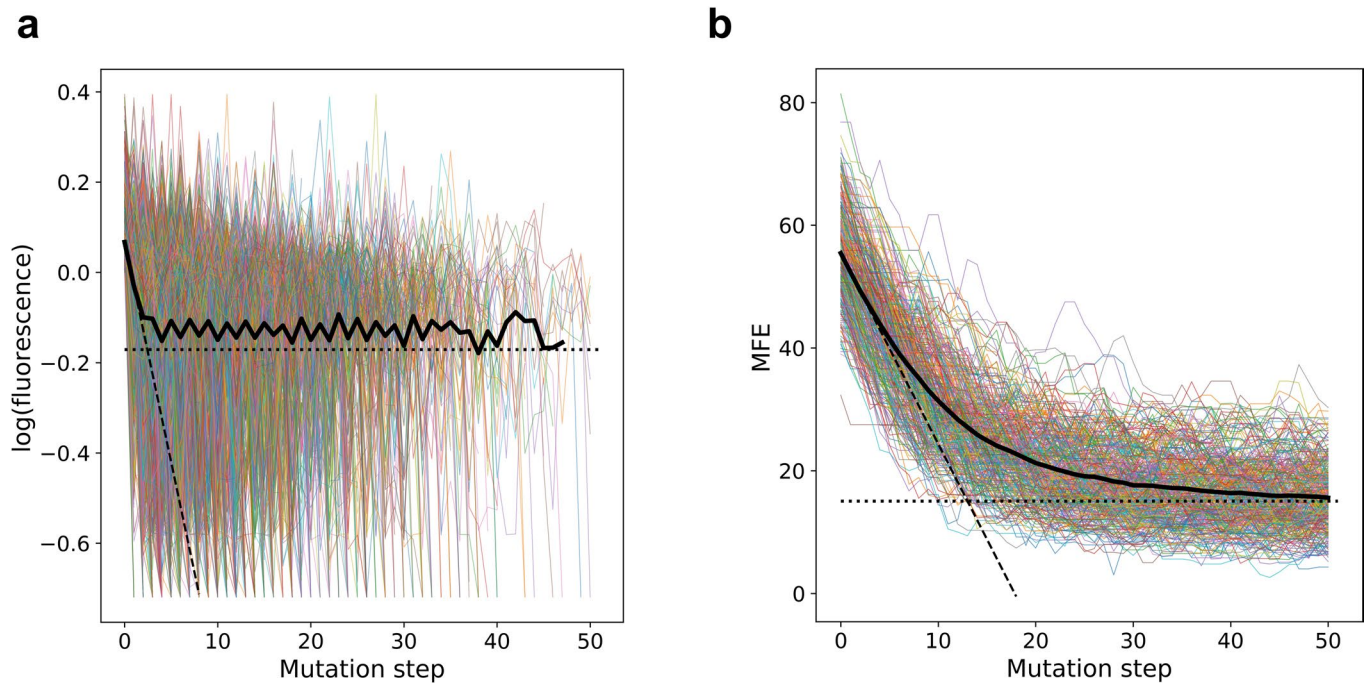
Extended Data Fig. 2 | Negative correlation between mutational effect and background phenotype in GFP and RNA stability landscapes. **a**, Distribution of Pearson's correlation coefficient (r) between mutational effect and background phenotype for individual mutations in the GFP landscape. **b**, Distribution of r for individual mutations in the RNA stability landscape. **c**, Relationship between background phenotype and mutational effect for all mutations in the GFP landscape. **d**, Relationship between background phenotype and mutational effect for all mutations in the RNA stability landscape. MFE, minimum free energy. The red line depicts the running mean in non-overlapping X-axis bins of width = 0.02 and 2 in (**c**, **d**), respectively, in all bins with more than 10 data points. There is no measurement error in the RNA stability landscape. Shared measurement error between mutational effect and background fitness cannot be controlled for in GFP as replicate fitness measurements are not available. For each mutation and its reverse, we considered a random one of them in (**c**, **d**).



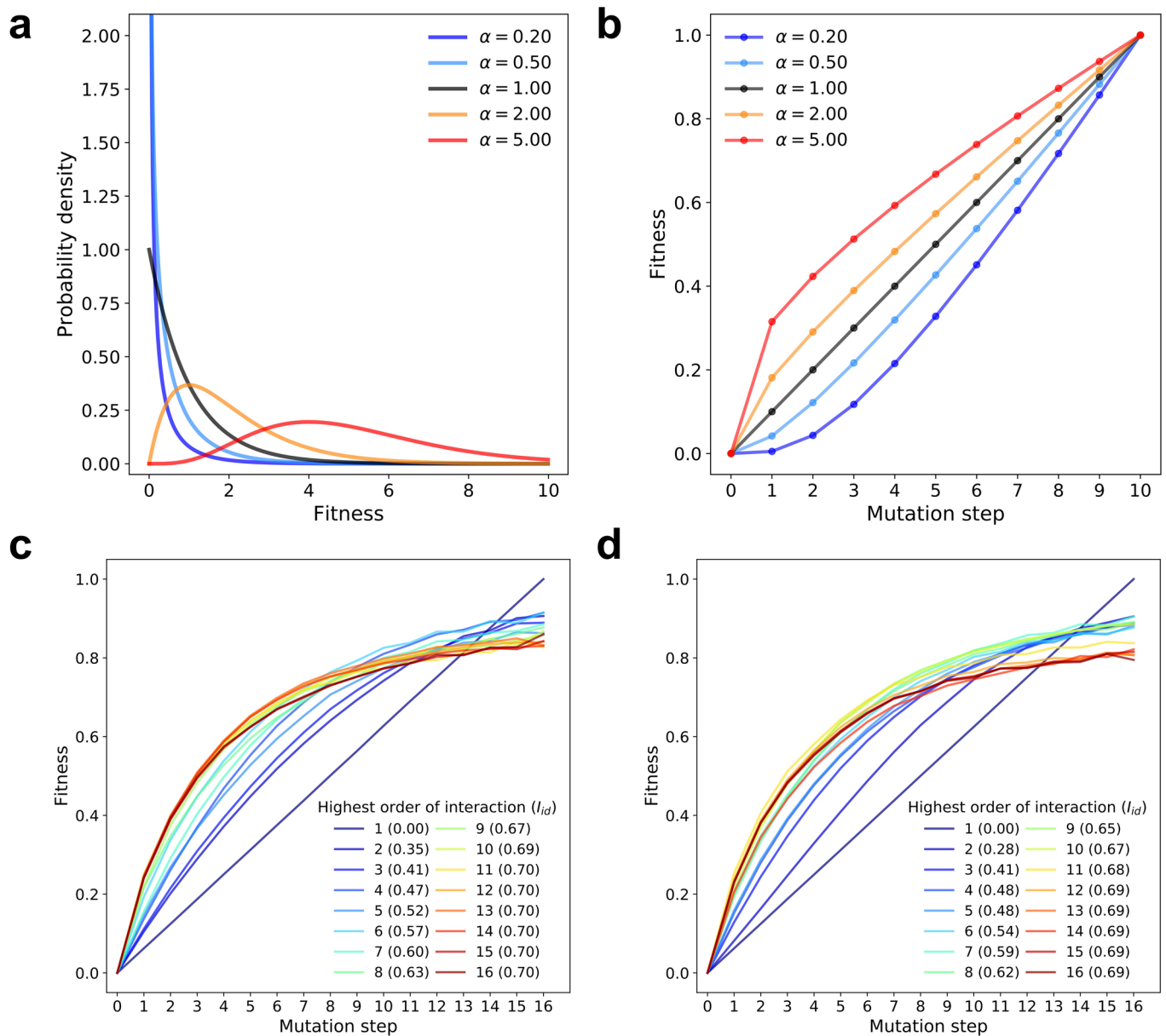
Extended Data Fig. 3 | Patterns of correlation between mutational effect and background fitness/phenotype for individual beneficial or deleterious mutations in various landscapes. **a**, Boxplots showing distributions of correlations in a series of n -order landscapes of 16 sites (where the highest order of nonzero interaction is indicated on the X-axis) for beneficial (blue) and deleterious (red) mutations, respectively. The lower and upper edges of a box represent the first (qu1) and third (qu3) quartiles, respectively, the horizontal line inside the box indicates the median (md), the whiskers extend to the most extreme values inside inner fences, $md \pm 1.5(qu3 - qu1)$, and the dots represent values outside the inner fences (outliers). **b-d**, Frequency distributions of correlations for individual beneficial mutations (blue) and deleterious mutations (red) in the tRNA (**b**), GFP (**c**), and RNA stability (**d**) landscapes. Whether a mutation is beneficial or deleterious is determined in reference to the wild-type (tRNA and GFP) or an arbitrary reference genotype (n -order and RNA stability). The wider distribution for deleterious than beneficial mutations is at least in part due to the larger number of deleterious than beneficial mutations.



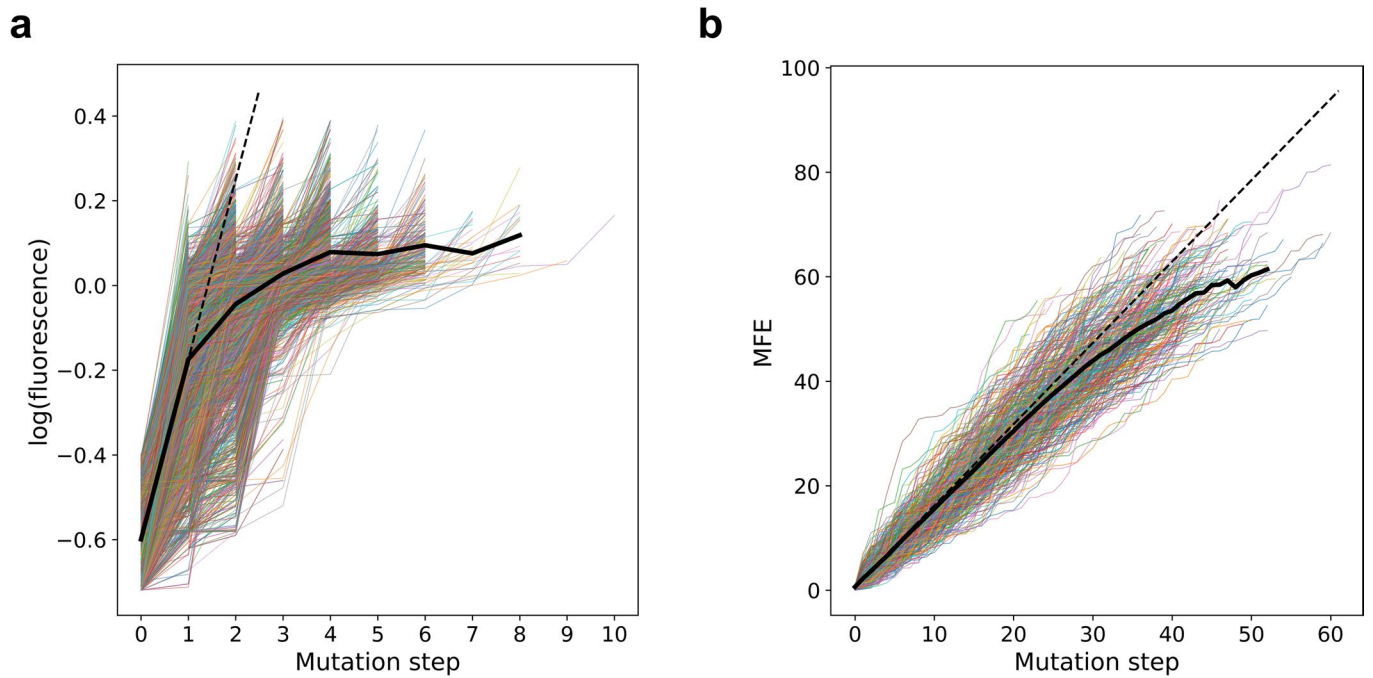
Extended Data Fig. 4 | Average fitness trajectories of mutation accumulation simulated in various n -order additive landscapes ($k = 1$) with different numbers of sites (n). The mean trajectories are scaled so that the minimum fitness appearing in the trajectory is 0 and the maximum is 1 to allow direct comparison.



Extended Data Fig. 5 | Fitness declines decelerate during mutation accumulation as a result of idiosyncratic epistasis. a, A total of 5000 fitness trajectories of mutation accumulation simulated in the GFP landscape, with the average trajectory shown in black, at each step when the trajectory number exceeds 10. **b,** A total of 350 fitness trajectories of mutation accumulation simulated in the RNA stability landscape, with the average trajectory shown in black. The dotted lines indicate the mean phenotypic value of all genotypes in the landscape, excluding non-active genotypes in the GFP landscape. For comparison, the dashed line in (a) or (b) represents the predicted linear decline given the slope in the first mutational step.



Extended Data Fig. 6 | Idiosyncratic epistasis is necessary but not sufficient to cause decelerating adaptations. **a**, Gamma distributions of genotype fitness for house-of-cards landscapes, with different values of the gamma shape parameter α . **b**, Theoretically computed mean fitness trajectories of adaptation on landscapes in **(a)** with corresponding colors. **c**, Average adaptive trajectories starting from the genotype with the lowest fitness (0), simulated in a series of n -order landscapes of 16 sites where each nonzero interaction term of each genotype is drawn from a gamma distribution of $\alpha = 1$. **d**, Average adaptive trajectories starting from the genotype with the lowest fitness (0), simulated in a series of n -order landscapes of 16 sites where each nonzero interaction term of each genotype is drawn from a beta distribution with $a=b=0.25$. For each landscape in **(c)** and **(d)**, the distribution of epistasis between mutations is symmetrical with mean equal to 0.



Extended Data Fig. 7 | Adaptation slows in empirical phenotype landscapes. **a**, A total of 5000 adaptive trajectories simulated in the GFP landscape, with the average trajectory shown in black, at each step when the trajectory number exceeds 10. **b**, A total of 350 adaptive trajectories simulated in the RNA stability landscape, with the average trajectory shown in black, at each step when the trajectory number exceeds 10. For comparison, the dashed line in **(a)** or **(b)** represents the predicted linear increase given the slope in the first mutational step.

Reporting Summary

Nature Research wishes to improve the reproducibility of the work that we publish. This form provides structure for consistency and transparency in reporting. For further information on Nature Research policies, see [Authors & Referees](#) and the [Editorial Policy Checklist](#).

Statistics

For all statistical analyses, confirm that the following items are present in the figure legend, table legend, main text, or Methods section.

n/a Confirmed

- The exact sample size (n) for each experimental group/condition, given as a discrete number and unit of measurement
- A statement on whether measurements were taken from distinct samples or whether the same sample was measured repeatedly
- The statistical test(s) used AND whether they are one- or two-sided
Only common tests should be described solely by name; describe more complex techniques in the Methods section.
- A description of all covariates tested
- A description of any assumptions or corrections, such as tests of normality and adjustment for multiple comparisons
- A full description of the statistical parameters including central tendency (e.g. means) or other basic estimates (e.g. regression coefficient) AND variation (e.g. standard deviation) or associated estimates of uncertainty (e.g. confidence intervals)
- For null hypothesis testing, the test statistic (e.g. F , t , r) with confidence intervals, effect sizes, degrees of freedom and P value noted
Give P values as exact values whenever suitable.
- For Bayesian analysis, information on the choice of priors and Markov chain Monte Carlo settings
- For hierarchical and complex designs, identification of the appropriate level for tests and full reporting of outcomes
- Estimates of effect sizes (e.g. Cohen's d , Pearson's r), indicating how they were calculated

Our web collection on [statistics for biologists](#) contains articles on many of the points above.

Software and code

Policy information about [availability of computer code](#)

Data collection

ViennaRNA (<https://www.tbi.univie.ac.at/RNA/>).

Data analysis

Custom code available at <https://github.com/lyonsdm/idiosyncrasy>

For manuscripts utilizing custom algorithms or software that are central to the research but not yet described in published literature, software must be made available to editors/reviewers. We strongly encourage code deposition in a community repository (e.g. GitHub). See the Nature Research [guidelines for submitting code & software](#) for further information.

Data

Policy information about [availability of data](#)

All manuscripts must include a [data availability statement](#). This statement should provide the following information, where applicable:

- Accession codes, unique identifiers, or web links for publicly available datasets
- A list of figures that have associated raw data
- A description of any restrictions on data availability

Code and new data are available at <https://github.com/lyonsdm/idiosyncrasy>.

Field-specific reporting

Please select the one below that is the best fit for your research. If you are not sure, read the appropriate sections before making your selection.

- Life sciences Behavioural & social sciences Ecological, evolutionary & environmental sciences

For a reference copy of the document with all sections, see nature.com/documents/nr-reporting-summary-flat.pdf

Life sciences study design

All studies must disclose on these points even when the disclosure is negative.

| | |
|-----------------|--|
| Sample size | This is a theoretical study with mathematical proofs, simulations, and data analysis. Sample size was based on the size of the available data. For one sample we created computationally, the sample size was 2 million. |
| Data exclusions | N/A |
| Replication | N/A |
| Randomization | N/A |
| Blinding | N/A |

Reporting for specific materials, systems and methods

We require information from authors about some types of materials, experimental systems and methods used in many studies. Here, indicate whether each material, system or method listed is relevant to your study. If you are not sure if a list item applies to your research, read the appropriate section before selecting a response.

Materials & experimental systems

| n/a | Involvement in the study |
|-------------------------------------|--|
| <input checked="" type="checkbox"/> | <input type="checkbox"/> Antibodies |
| <input checked="" type="checkbox"/> | <input type="checkbox"/> Eukaryotic cell lines |
| <input checked="" type="checkbox"/> | <input type="checkbox"/> Palaeontology |
| <input checked="" type="checkbox"/> | <input type="checkbox"/> Animals and other organisms |
| <input checked="" type="checkbox"/> | <input type="checkbox"/> Human research participants |
| <input checked="" type="checkbox"/> | <input type="checkbox"/> Clinical data |

Methods

| n/a | Involvement in the study |
|-------------------------------------|---|
| <input checked="" type="checkbox"/> | <input type="checkbox"/> ChIP-seq |
| <input checked="" type="checkbox"/> | <input type="checkbox"/> Flow cytometry |
| <input checked="" type="checkbox"/> | <input type="checkbox"/> MRI-based neuroimaging |